doi:10.36487/ACG_repo/2435_D-08
9th International Conference and Exhibition on Mass Mining, Kiruna Sweden 17-19 September 2024

A review of the mining adjustments to the In-situ Rock Mass Rating (IRMR) through a sensitivity analysis using Finite/Discrete Element Method

H. Pichuante[a,b], J. Jakubec[b], A. Thomas[b] and D. Elmo[a]
[a]*University of British Columbia, Vancouver, Canada*
[b]*SRK Consulting, Vancouver, Canada*

ABSTRACT

One of the main challenges of caving projects is the realistic prediction of the undercut dimension at which caving will initiate and propagate. To address this need, empirical approaches were proposed, such as the cavability chart published by Diering & Laubscher (1987), which is based on the hydraulic radius and Modified Rock Mass Rating. Furthermore, the rock mass classification system used has limitations and is open to subjectivity, mainly due to its "mining adjustment factors" to convert In-situ Rock Mass Rating into Modified Rock Mass Rating. This study consists of a sensitivity analysis using a series of Finite-Discrete Element Models to evaluate the response of different conceptual rock masses characterized by the In-situ Rock Mass Rating system. These rock masses were assessed under different in-situ stress regimes and discontinuity arrangements to investigate the influence of these parameters on cave initiation and propagation. The results were compared with the most recent version of the Modified Rock Mass Rating system and its related cavability chart. This showed a poor match when comparing empirical predictions with the numerical model results under a low in-situ stress ratio, which means a higher adjustment must be applied for these cases, while a better agreement was observed for stress ratios between 1.5 to 2.5.

1 INTRODUCTION

One of the first attempts to predict the cavability of a deposit was proposed by Laubscher (Diering & Laubscher 1987, Laubscher 1990, 1994, 2000), using an empirical method based on the Modified Rock Mass Rating (MRMR) system and the hydraulic radius (HR). Laubscher's stability chart, also found in the literature as cavability chart (Figure 1), after more than 30 years, and even when some questions have arisen, remains one of the standard methods used by the industry for the early stages of a project.

From the two components used by the empirical method, HR is defined as a measure of the shape of the planned excavation geometry, and it is calculated by dividing the area of the face of the excavation by its perimeter. The MRMR system, unlike the other most used classification systems (Figure 2), was mainly developed for mining applications and cavability assessment by Laubscher (1975, 1990) and Laubscher & Jakubec (2001). The MRMR is calculated by applying different mining adjustment factors to the in-situ rock mass rating or "IRMR" (Laubscher & Jakubec, 2001).

From the list of mining adjustments proposed by Laubscher, the same author described the stresses and joint orientation as critical parameters for the stability of the cave back. However, these adjustments have been considered one of the main limitations of the MRMR system due to the lack of detailed guidelines to apply these factors, leading to subjective misuse (Truman & Mawdesley, 2003), especially in the case of adjustment by stresses.

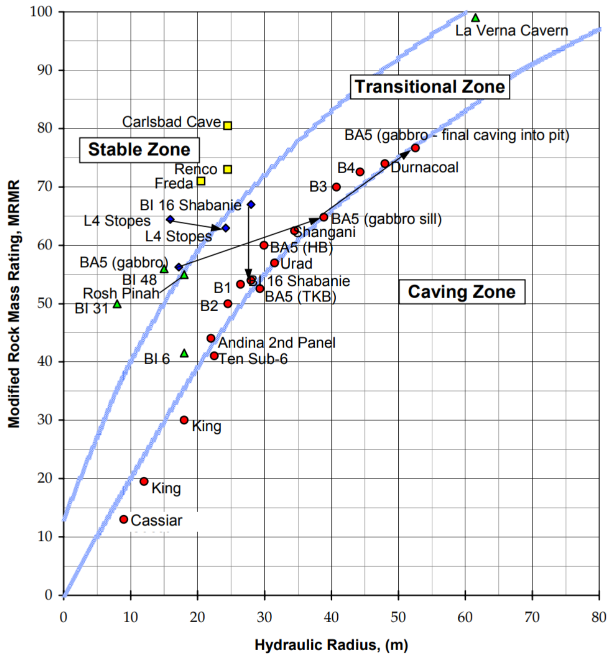

Figure 1 Laubscher's cavability chart (after Laubscher, 1994).

It is well known that the stresses induced around mining excavations significantly influence their stability and cave propagation. The stress field changes as the cave propagates upwards and is influenced by factors such as the in-situ stress field, the initial topography, the rock mass structure, and other excavations (Suzuki, 2019).

Nevertheless, in-situ stresses are considered one of the most critical factors affecting induced stresses since they dictate the nature of the stress redistribution around the undercut excavation.

To assess the influence of in-situ stresses and joint orientation on cave initiation and propagation, a series of two-dimensional finite-discrete element models (FDEM) coupled with a simplified discrete fracture network (DFN) were created using the software ELFEN (Rockfield, 2011). This paper presents the results of these models that enabled the investigation of cavability under different conceptual rock masses characterized by the IRMR system. As a result, it was possible to critically review the most controversial adjustment factors used by the latest version of the MRMR system.

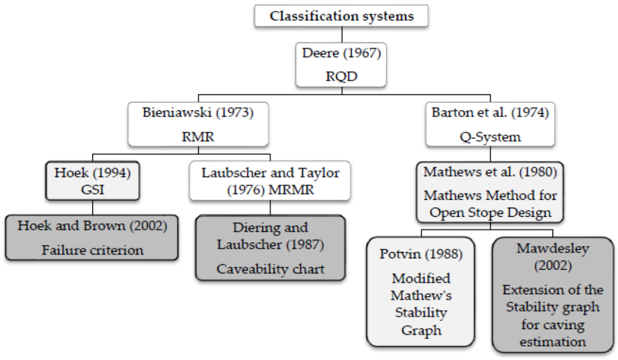

Figure 2 Empirical methods used in block caving mines (Suzuki, 2019).

2 MODEL SETUP

The code ELFEN is a 2D/3D numerical modelling package incorporating hybrid FEM/DEM techniques with fracture capability that has recently found increasing use in rock mechanics (Elmo et al., 2010). There are several examples in the literature of block cave modelling in ELFEN, including Elmo et al. (2008, 2010, 2022), Pine et al. (2007), Vyazmensky (2008) and Shapka-Fels (2022).

In this research, a series of conceptual 2D FDEM-DFN models were designed to investigate the differences in outcomes depending on the selected rock mass classification method (IRMR) and modelling assumptions. In particular, the effects of material properties, the presence of discrete fractures and patterns, and in-situ stresses, among others, were examined. As shown in Figure 3, the dimension of the model is 2,850 m × 1,200 m, subdivided into elastic and elastoplastic regions with fracturing. The non-fracturing elastic region is required to minimize boundary effects and is modelled with a lower mesh resolution (50 m near the model boundaries). Near the undercut level (UCL) within the plastic zone, it was modelled with a higher mesh resolution ranging from 2-8 meters. The model comprises an UCL of 5 meters in height located 1,000 m below the ground surface. The UCL used for the sensitivity analysis was 80, 120 and 160 meters wide, equivalent to a HR of 20, 30 and 40 meters, respectively, when assuming a square layout.

The undercut level was excavated using multiple stages (4-6 depending on the HR).

The DFN components were modelled in FracMan (WSP, 2023) to create the different 3D models and export them as 2D sections. More details of the integrated use of ELFEN and FracMan can be found in Elmo et al. (2006) and Pine et al. (2007). Two different discontinuity arrangements were modelled using two joint sets: DFN1 includes a horizontal and vertical set, and DFN2 includes joints with 30 and 60 degrees dipping in the same direction. Both scenarios assumed joint persistence of 30 meters and spacing of 15 meters.

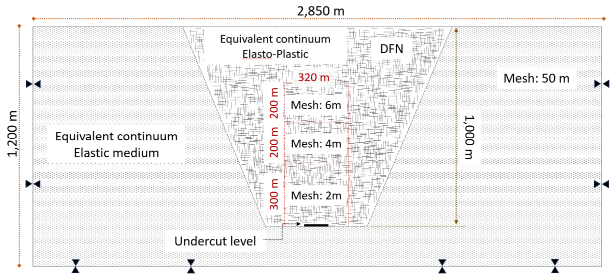

Figure 3 Model geometry and basic setting.

2.1 Simulation of the mining process in ELFEN

FDEM are computed using incremental numerical time steps. Model time is described in seconds, and stages are defined to initiate and terminate at specific times or a particular number of time steps. All the models presented in this paper used excavation sequences that go from left to right, followed by a uniform draw sequence, which was set as an algorithm for element deletion every two seconds.

For the undercut excavation and draw simulation in ELFEN models, the approach described in Elmo et al. (2010) was implemented for the current analysis. According to this methodology, ore is removed across the assumed production level using a specific algorithm that eliminates all the meshed elements whose centroids are located within a specified region (Figure 4). When the area has been defined, the ore is removed continuously at a given numerical time step.

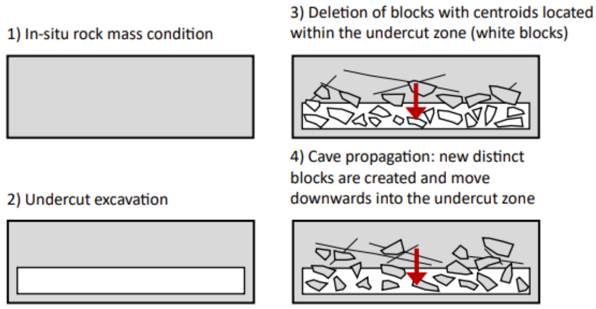

Figure 4 ELFEN deletion methodology (Shapka-Fels & Elmo, 2022).

2.2 Rock mass properties for sensitivity analysis

2.2.1 Rock Mass Classification

Although this study was mainly conceptual, a real field database was used to define the different rock masses and correlations between systems. The database consisted of more than 2,000 meters of detailed geotechnical core logging collected to calculate in-situ rock mass rating (IRMR) and Rock Mass Rating (RMR89, Bieniawski, 1989) systems. The data were collected from an undisclosed project that is currently evaluating the option of a mass mining method.

As illustrated in Figure 5, the core logging data was utilized to correlate IRMR and the Geological Strength Index (GSI, Hoek et al., 2013), the latter calculated based on the RQD and the joint condition from RMR89. Despite the inherent differences between the two systems, a clear trend was found, and the two best curve fits have been analyzed, a linear and an exponential regression. As expected, the differences between both curves increase to the extreme sides. From this graph, the dispersion of the data could be explained for the different parameters considered by each system. While GSI uses fracturing (from the RQD parameter) and joint condition (JC_{B89}), the IRMR system uses rock strength, joint spacing and joint condition but additionally incorporates rock defects to adjust the rock strength and cemented joints to change the joint spacing.

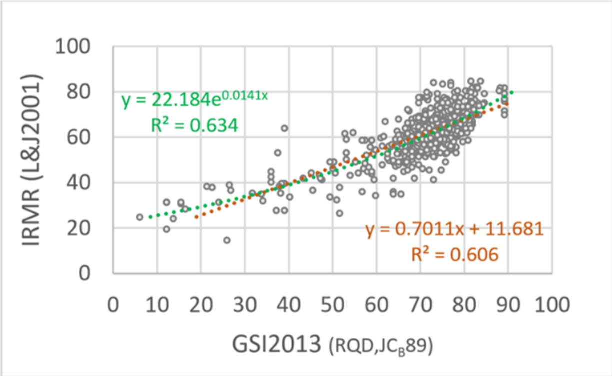

Figure 5 IRMR-GSI correlation using 2000 meters of core logging from an undisclosed project.

For both fit, higher values of IRMR compared to GSI are identified for a poor rock mass (IRMR<30), while lower values of IRMR than GSI were found for stronger rock masses (IRMR>55). For this analysis, the exponential fit was considered more appropriate for limiting the maximum values of GSI due to the presence of defects and cemented joints in strong rock masses.

This assessment considers five different rock masses classified with their IRMR values and equivalent GSI. The *UCS* and m_i were selected using field data and adjusted correctly with a literature review to represent each rock mass. The properties used to define the Hoek-Brown failure envelopes and later their equivalent Mohr-Coulomb properties are presented in Table 1.

2.2.2 Rock Mass Properties

The material was modelled using a Mohr-Coulomb with Rankine rotating crack tensile cut-off constitutive model in ELFEN code. A detailed explanation of these models can be found in Klerck (2000) and Elmo (2006).

The material parameters required for ELFEN numerical analysis have been derived from empirical relationships based on rock mass classification systems.

Table 1 Conceptual rock masses and their basic properties.

Rock Mass	*UCS* (MPa)	IRMR	GSI	m_i
RM-1	60	35	32	12
RM-2	80	45	50	14
RM-3	100	55	64	16
RM-4	140	65	76	18
RM-5	160	75	86	20

Rock mass internal cohesion and friction angle were estimated using the approach proposed by Hoek et al. (2002), assuming specific values for the parameter m_i and a $\sigma 3_{max}$ value of 13 MPa. A Poisson's ratio of 0.25 was selected for this analysis, and the values of Young's Modulus for the rock mass (E_{rm}) were calculated using the equation proposed by Hoek & Diederichs (2006). The rock mass tensile strength (σ_{tm}) was assumed to be 75% of the theoretical value calculated using the Mohr-Coulomb criterion. Fracture energy (G_f) was calculated using the equation proposed by Klerck (2000), while dilation (ψ) was estimated using Hoek & Brown's (1997) approach.

The models showed to be sensitive to σ_{tm} and E_{rm}. For example, unreliable crack initiation was observed when using Mohr-Coulomb tensile strength with no calibration. It is similar to defining Young's modulus as the poorest rock mass. Since this modulus from empirical calculation was too low, it led to significant and unrealistic deformation areas with scarce crack initiation. The summary of properties for each of the five conceptual rock masses is presented in

Table 2.

Table 2 Rock mass properties defined for the five conceptual rock masses.

Rock Mass parameter	Unit	RM-1	RM-2	RM-3	RM-4	RM-5
GSI	-	32	50	64	76	86
Young's Modulus (E_{rm})	MPa	8,686	17,372	21,650	40,869	52,459
Poisson's ratio (ν)	-	0.25	0.25	0.25	0.25	0.25
Tensile Strength (σ_{tm}) (1)	MPa	1.68	2.27	2.86	3.88	5.37
Cohesion (c)	MPa	1.9	3.1	4.6	7.3	11.1
Friction Angle (ϕ)	degrees	29	38	45	51	54
Fracture Energy (G_f)	$J\ m^{-2}$	23.6	23.1	22.1	24.5	22.6
Dilation (ψ)	degrees	7	10	11	13	14

The shear strength properties assigned to the discontinuities are defined according to the Mohr-Coulomb criterion; a friction angle of 35 degrees and zero cohesion were used. The other additional parameters required by ELFEN, such as normal (P_n) and tangential penalties (P_t), were estimated using the recommendations provided in Elmo (2006) and the ELFEN user manual (Rockfield, 2011), as presented in Table 3.

Table 3 ELFEN modelling input parameters for existing and new structures.

Structures - Properties	Unit	Joints and new fractures
Fracture Friction	degrees	35
Facture Cohesion (c)	MPa	0
Normal Penalty (P_n)	GPa m^{-1}	5
Tangential Penalty (P_t)	GPa m^{-1}	0.5
Tensile Strength (s_t)	MPa	0

3 SENSITIVITY ANALYSIS

The effect of in-situ stresses on cavability was evaluated through a sensitivity analysis using FDEM-DFN for each of the five rock masses. While the rock mass properties were held constant, two different DFN models were assessed. The first DFN model considers two joint sets, one horizontal and one vertical (DFN1), and the second DFN model includes two joint sets but with inclinations of 30 and 60 degrees (DFN2) dipping in the same direction. Another variable of the analysis was the dimension of the undercut level. Since all the FDEMs were 2D, a square footprint shape was assumed for each case. The dimensions of the selected UCL are 80 meters, 120 meters and 160 meters wide, corresponding to hydraulic radii of 20, 30 and 40 meters respectively. This implies that for each in-situ stress scenario to be evaluated, there would be 15 different models when combining five-rock masses and three hydraulic radii as variables for the same DFN. The in-situ stresses were simplified for modelling using the horizontal-to-vertical stress ratio (K-ratio). Different ratios were applied, keeping the other properties/parameters constant. To select the K-ratio for the sensitivity analysis, the observations presented by Flores & Karzulovic (2003) were considered, and ratios of 0.5, 1, 1.5, 2 and 2.5 were applied.

Laubscher's cavability chart was utilized to summarize the different models used for the analysis. Figure 6 illustrates all the various scenarios regarding rock mass quality and HR run for each stress regime and DFN configuration. This plot enables the comparison between the empirical method and the FDEM results. For this study, the base cases would consider the MRMR values equal to the IRMR. No adjustment factors have been applied to define the different rock mass properties.

The same criteria used by Laubscher (2000) to describe the three caving states in the cavability chart were applied in this study, "Caving" when caving occurs and is followed by self-sustained propagation. "Transitional" when the cave initiates, but propagation is minimal, and "Stable."

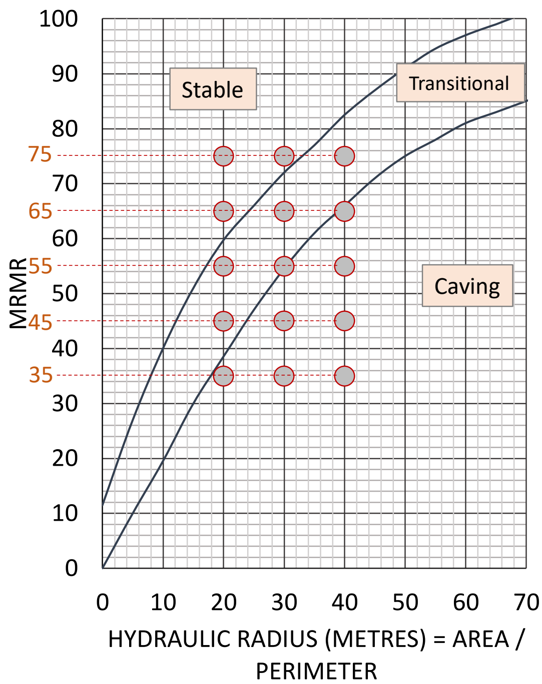

Figure 6 Different scenarios modelled for sensitivity analysis and plotted on Laubscher's cavability chart.

As this work aims to assess cavability by determining if caving continues to propagate after its initiation, projecting the entire cave to the surface is unnecessary. Instead, a fixed extraction area has been established for all the models to ensure comparability. Computational resources also influenced this decision. Without this consideration, the study would be impractical due to the many models needed for the sensitivity assessment.

3.1 Sensitivity analysis results

This section analyzed and discussed the results of the multiple models created to explore the rock mass response to different stress regimes. The results for each model, in terms of vertical deformation are summarized in Figure 7. However, due to the large number of models, only the caving illustration of two representative cases (K-ratio 1 and 2) is presented in this paper.

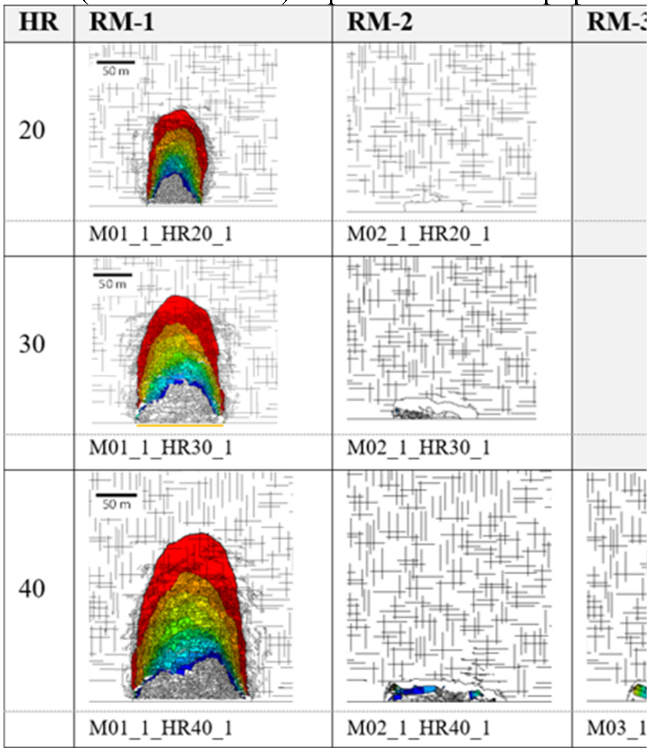

Figure 8 and Figure 9 present the models with DFN1, and Figure 10 and Figure 11 for models with DFN2.

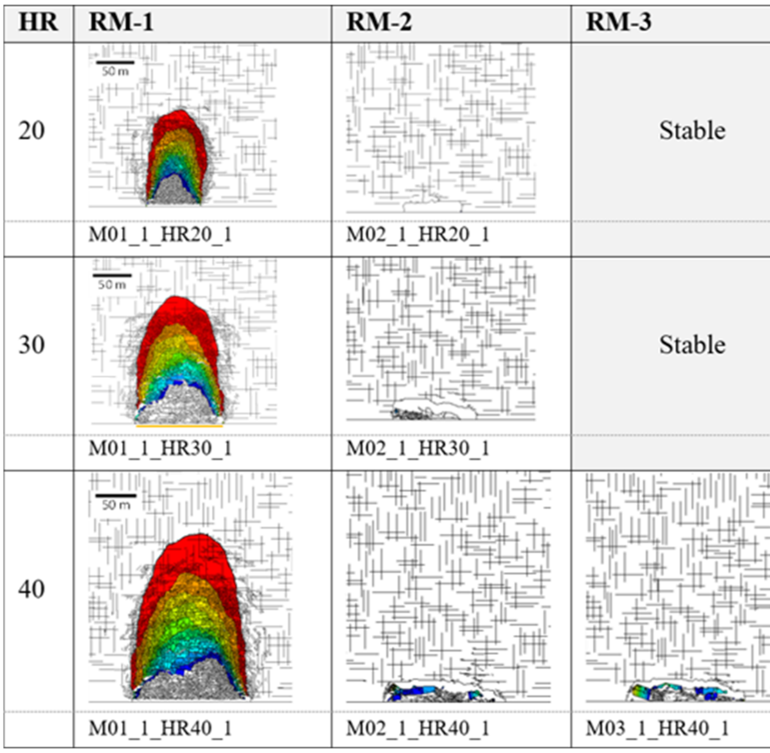

Figure 8 shows the case result using an in-situ stress ratio of 1. The vertical stress has been defined as gravitational loading with a rock unit weight of 0.026 MN/m^3 and the UCL located at a depth of 1,000 meters. The initial major principal stress is equivalent to 26 MPa, and the same stress is expected for the horizontal component. Under this stress regime, most rock masses remain stable (RM-4 and RM-5) or present initial failures but do not propagate (transitional state) like RM-2 and RM-3. The exception was observed for the weakest rock mass (RM-1), which shows caving propagation. As expected, when comparing the extension of the vertical deformation for the same rock mass and stress regime, it increases with the HR (Figure 7).

Figure 9 shows the results for an in-situ stress ratio of 2, and a different rock mass response can be observed. In terms of cavability, it increases with HR and also due to the effect of high horizontal stress compared to the previous scenario. Under the same HR, stronger rock masses transition from the "stable" to the "caving" stage as the K-ratio increases. Additionally, as illustrated in Figure 7, the vertical deformation increases for the different rock masses as the stress regime increases, and a direct relation between vertical deformation in stronger rock masses (RM-3, RM-4) can be observed. The increase in horizontal stress also increases crack initiation and distribution around the cave zone. These newly formed cracks seem to potentiate cave propagation and might reduce the risk of cave stalling. In

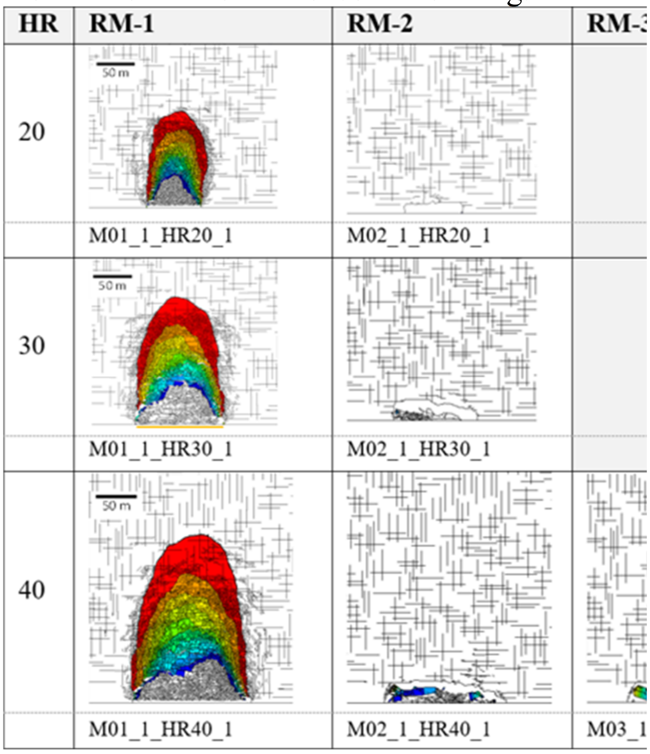

Figure 8 to Figure 11, the red colour represents a vertical displacement within a 1-2 meter range. This means that in the case of displacement, all the cracks above and around this red band are less than one meter in the y-axis. However, as the material extraction continues, those cracks start opening, and new blocks move downwards.

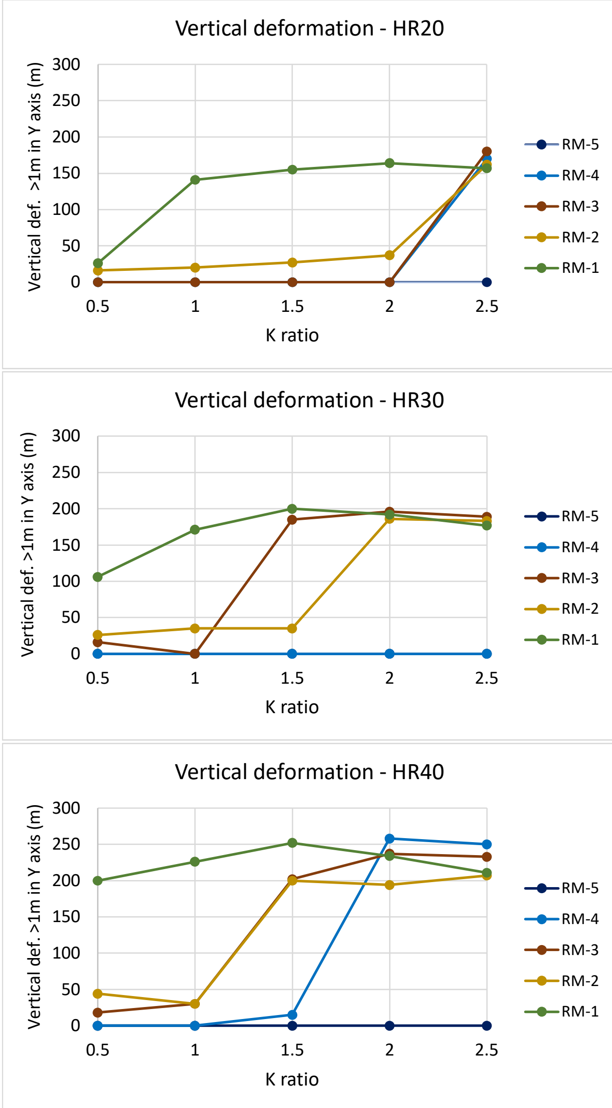

Figure 7 Graphs showing vertical deformation using DFN1 under various stress regimes. Upper: HR of 20m, after ~1500m^2 extraction. Center: HR of 30m and, lower: 40m after ~2500m^2 extraction (for instances of caving).

The case of RM-5, under all the different HR and stress scenarios, remains stable, with no cave initiation observed. To assess the cavability of this strong rock mass, a larger HR would need to be modelled.

A second batch of models using the same rock masses and stress regimes was evaluated using the "DFN2" configuration featuring two joint sets dipping at 30 and 60 degrees. The results of these analyses are presented in Figure 10 for a stress ratio of 1 and Figure 11 for a stress ratio of 2.

For a K-ratio of 1, caving is restricted to the weakest rock mass (RM-1) with HR of 30 and 40m. RM-2 only caves with HR of 40, but the propagation seems more limited. The models with an HR of 20m remain stable, even for the weakest rock mass.

When the K-ratio is increased (K-ratio 1.5 or 2), it potentiates cavability and extends for stronger rock masses, but only when the HR is 40m (Figure 11). Finally, when the K-ratio is increased to 2.5, stronger rock masses (RM-2 and RM-3) start to cave under an HR of 30m. Similar to the observations made for models using DFN1, under high K-ratio, the initiation of new cracks increases and expands upwards for the strong rock masses.

Now, when comparing both DFN scenarios (DFN1 and DFN2), there is an apparent increase in cavability for DFN1 (0-90 degrees). Several cases that were classified as “caving stage” when the models were run with DFN1 were later categorized as “stable” or “transitional” when using DFN2. This difference is more evident under high K-ratios.

The extension of the vertical deformation also propagates further up for DFN1 models compared to those using DFN2. The fact that DFN2 includes two sets dipping in the same direction, far from perpendicularity, appears to be one of the reasons for the difference in cavability. A good example can be seen when comparing the model “M02_1_HR30_2” with “M02_2_HR30_2”.

The results indicate a more favourable condition when the rock mass combines horizontal and vertical join sets. This aligns with Kendorski's (1978) and Flores & Karzulovic's (2003) observations about cave initiation and propagation and the need for a low-dipping joint set to be successful, with the most favourable condition to occur when this low-angle joint set is intercepted by two sub-vertical sets, creating favourable conditions for the vertical displacement of the blocks. Karzulovic (2001) also described that sub-horizontal joint sets are expected to be more relevant during caving initiation, while joints with higher dips during cave propagation.

Regarding cave propagation, for models using DFN1, the deformation and propagation of the fractured zone are generally isometric and extend vertically above the UCL. However, in the same scenarios but using DFN2, there tends to be an inclination of the cave propagation to one of the sides of the UCL. In this case, to the left, where both joint sets are dipping. Similar observations were described by Elmo et al. (2007) and Vyazmensky (2008). The work of Vyazmensky (2008) discusses in detail how vertical to steeply dipping joints govern the direction of cave propagation. The shallower the dip of these joints, the more inclined the cave propagation direction is from vertical.

4 FDEM RESULTS COMPARED WITH LAUBSCHER’S CAVABILITY CHART

Since the different rock masses modelled for the sensitivity analysis were initially defined from the IRMR system, comparing results from the FDEM and the curves from the cavability chart proposed by Laubscher (2000) is possible. Each of the ELFEN model results was analyzed and classified within the three possible stages: “Caving,” “Transitional,” and “Stable,” and plotted in Laubscher’s chart. One chart contains 15 model results for a specific stress regime.

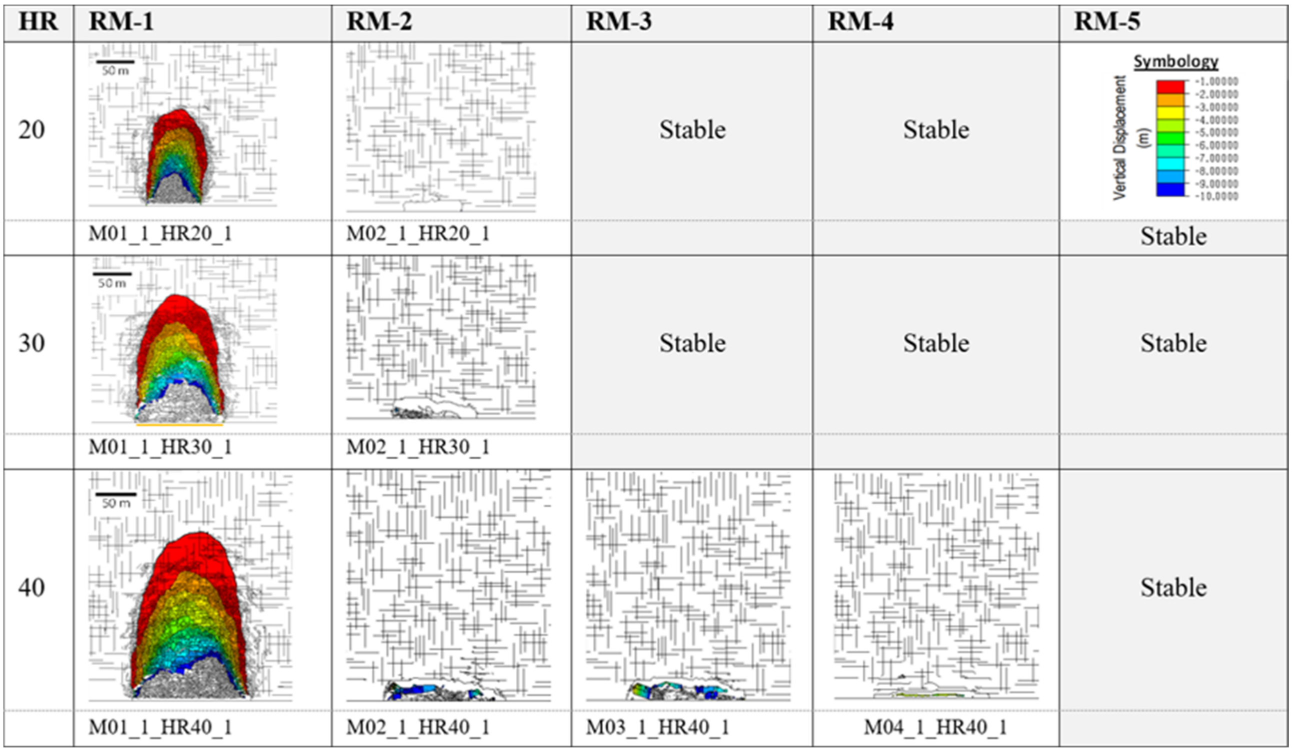

Figure 8 Models for cavability assessment of different rock masses using DFN1, under K-ratio of 1. Models with HR of 20m were analyzed after ~1500m^2 extraction, while models with HR of 30 and 40m were analyzed after ~2500m^2 extraction (for instances of caving).

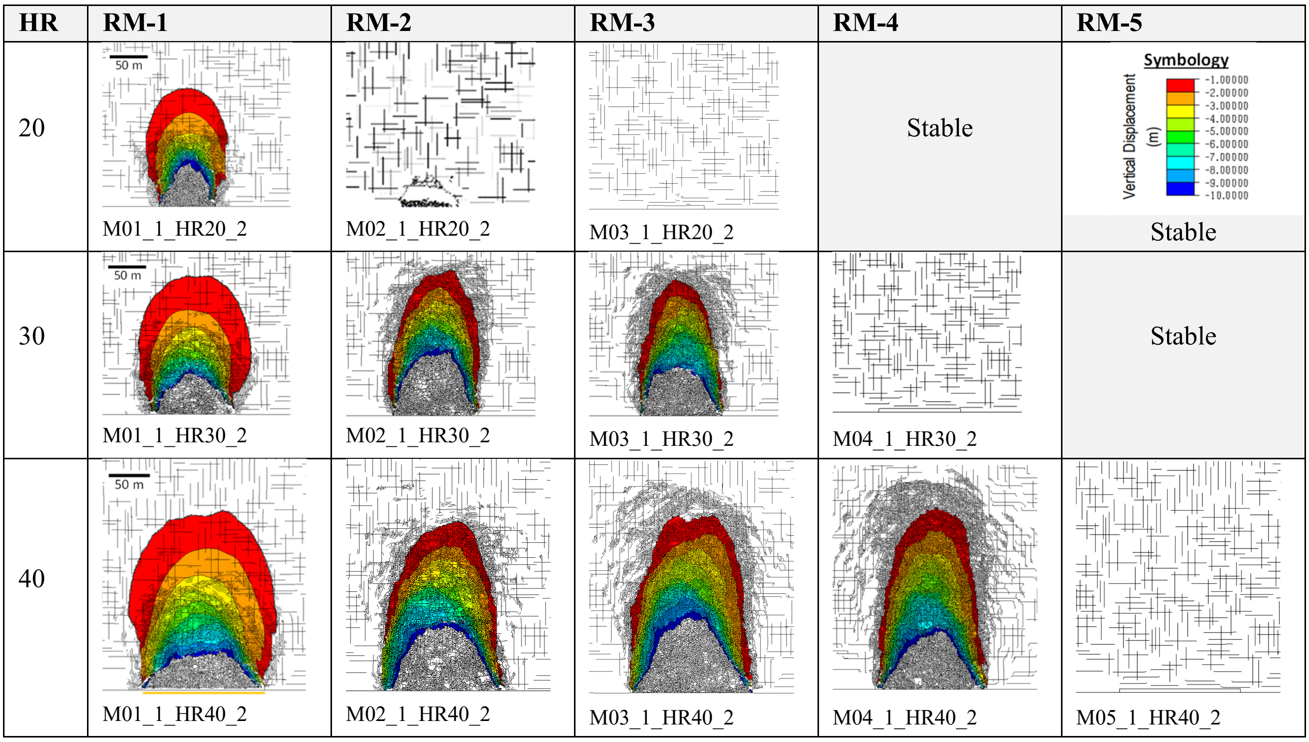

Figure 9 Models for cavability assessment of different rock masses using DFN1, under K-ratio of 2. Models with HR of 20m were analyzed after ~1500m^2 extraction, while models with HR of 30 and 40m were analyzed after ~2500m^2 extraction (for instances of caving).

HR	RM-1	RM-2	RM-3	RM-4	RM-5
20	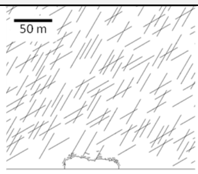 M01_2_HR20_1	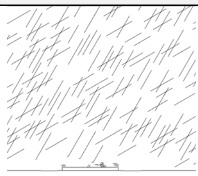 M02_2_HR20_1	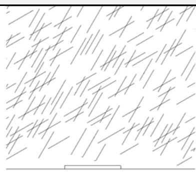 M03_2_HR20_1	Stable	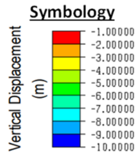 Stable
30	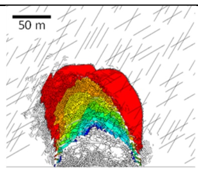 M01_2_HR30_1	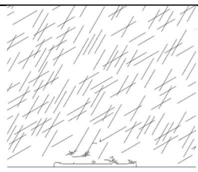 M02_2_HR30_1	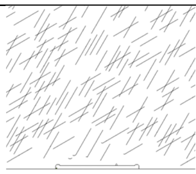 M03_2_HR30_1	Stable	Stable
40	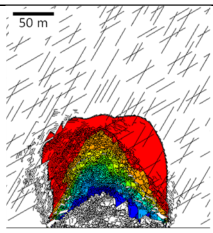 M01_2_HR40_1	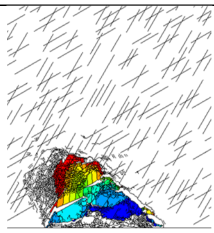 M02_2_HR40_1	 M02_2_HR40_1	Stable	Stable

Figure 10 Model for cavability assessment of different rock masses using DFN2, under K-ratio of 1. Models with HR of 20m were analyzed after ~1500m² extraction, while models with HR of 30 and 40m were analyzed after ~2500m² extraction (for instances of caving).

HR	RM-1	RM-2	RM-3	RM-4	RM-5
20	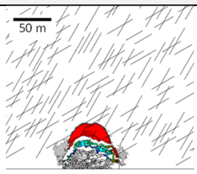 M01_2_HR20_2	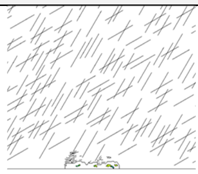 M02_2_HR20_2	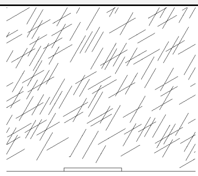 M03_2_HR20_2	Stable	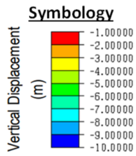 Stable
30	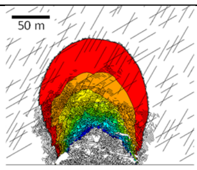 M01_2_HR30_2	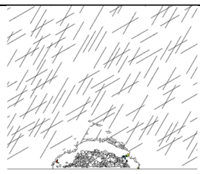 M02_2_HR30_2	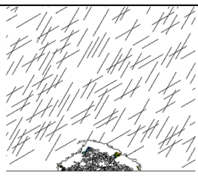 M03_2_HR30_2	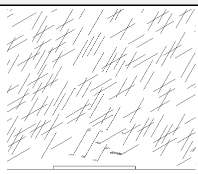 M04_2_HR30_2	Stable
40	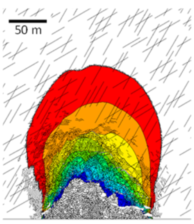 M01_2_HR40_2	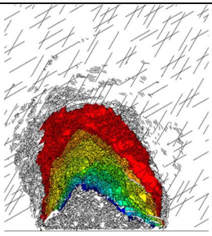 M02_2_HR40_2	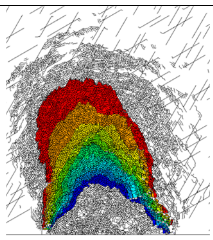 M03_2_HR40_2	 M04_2_HR40_2	Stable

Figure 11 Model for cavability assessment of different rock masses using DFN2, under K-ratio of 2. Models with HR of 20m were analyzed after ~1500m² extraction, while models with HR of 30 and 40m were analyzed after ~2500m² extraction (for instances of caving).

Error! Reference source not found. summarizes the results for each model coupled with DFN1 and Figure 13 models with DFN2. Generally, the models associated with DFN1 present a poor correspondence with the empirical prediction when the stress ratio is low (0.5 and 1). However, it improves with the increase in the stress ratio (1.5, 2 and 2.5). The in-situ stress ratio of 2 shows the best match with the empirical curve for the caving prediction; nevertheless, the “transitional” stage was not typical in the FDEM for high stresses, and it was more abundant in those models with low K-ratio.

For models coupled with DFN2 (Figure 13), a poorer correlation with the empirical prediction can be described. Caving is more restricted to the weakest rock mass under a low-stress ratio, while for a high-stress ratio, caving is mainly related to HR 40m. Unlike the results using DFN1, the models present more “transitional” stages for high-stress ratios.

Under a general view of the results, the poor match under a low stress ratio is an interesting finding, considering that the initial concept of the Laubscher chart is based mainly on cases under the South African stress regime, where the major principal stress is commonly assumed to be vertical and the intermediate and minor stresses are horizontal. However, the numerical models showed something different, and for cases when gravitational caving (low K-ratio) was expected, there was not a good fit to the empirical curve; instead, a better agreement was seen for stress-induced caving (high K-ratio).

Aligned with this observation, one of the main limitations that several authors have described to Laubscher’s chart is that there is no justification for the position of the caving boundary for values of MRMR higher than 50, which may be flatter than indicated (Lorig et al., 1995; Mawdesley, 2002). On the other hand, Truman & Mawdesley (2003) recommended that for specific cases where Laubscher’s empirical method has been applied in moderately strong to strong rock masses under low/moderate stresses, the undercut dimensions to induce continuous caving may be significantly greater than predicted by the chart.

The results of this study also suggest the need to flatten the empirical curve for strong rock masses under low stress ratio or, in other words, use greater HR under this stress regime. Another option would be to modify the adjustment factors applied to the IRMR when using the empirical chart.

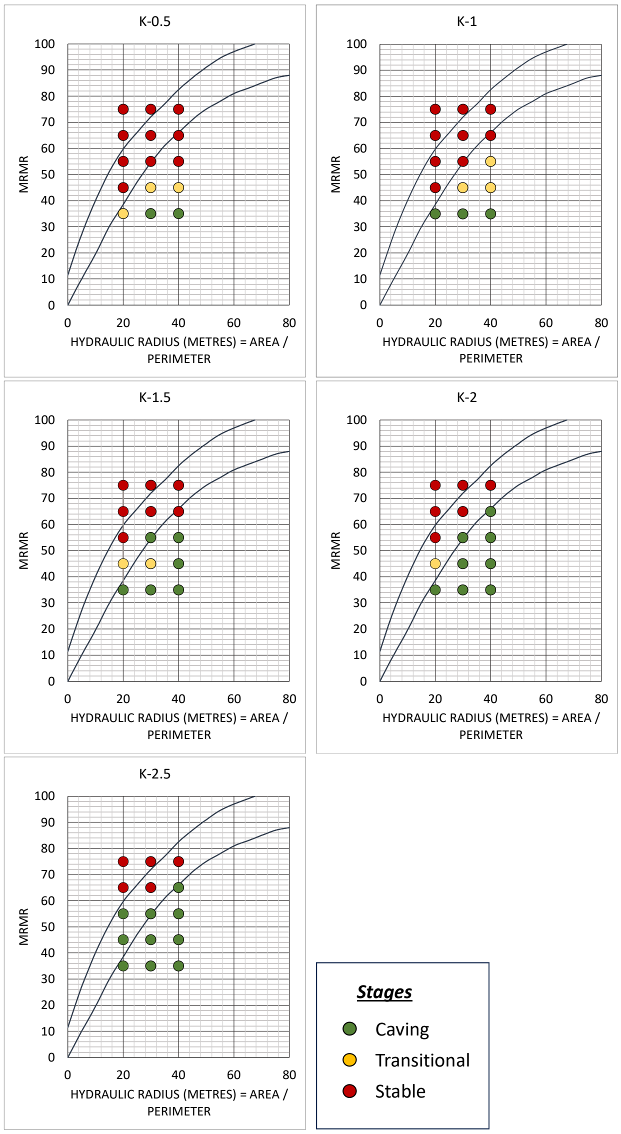

Figure 12 Laubscher’s chart showing the FDEM results of cavability analysis for models using DFN1 (joint sets 0-90 deg.) under different K-ratio.

4.1 Stresses Adjustment Factors to IRMR

Based on the FDEM results and the comparison discussed in the previous section, a simple conceptual adjustment curve for the in-situ stresses is presented. As different rock masses' responses to cavability were seen depending on the structural arrangement, two curves have been plotted to account for these various configurations.

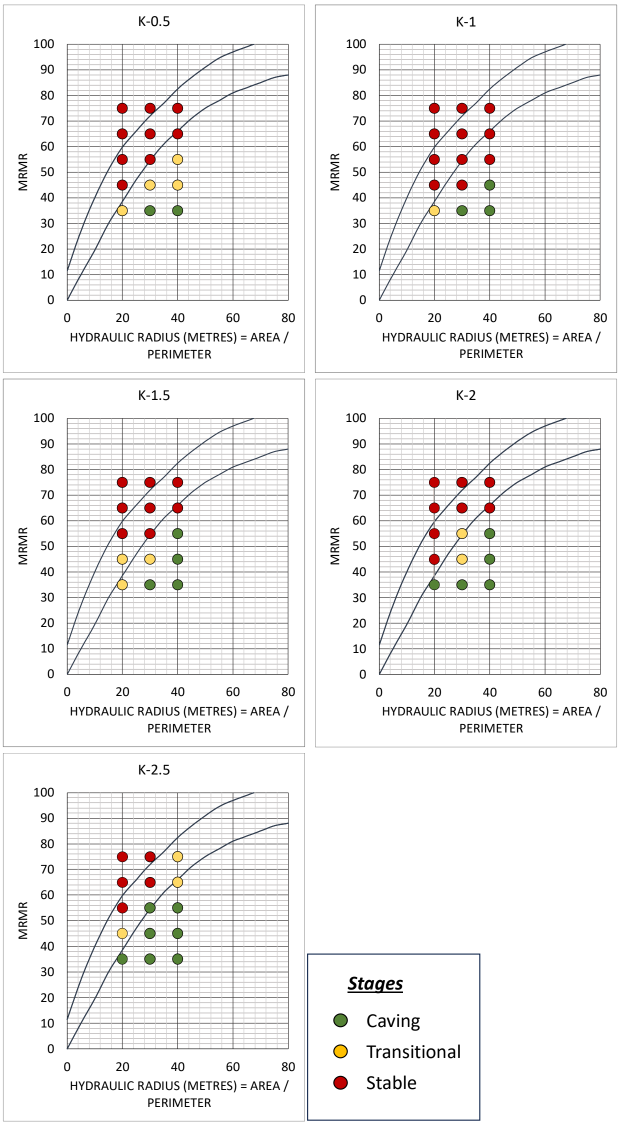

Figure 13 Laubscher's chart showing the FDEM results of cavability analysis for models using DFN2 (joint sets 30-60 deg.) under different K-ratio.

Figure 14 presents the adjustment to obtain the MRMR depending on the in-situ stress ratio acting on the rock mass. When the most favourable joint sets are present (sub-horizontal and sub-vertical sets), the adjustment for low stress ratio will tend to increase the MRMR rating, meaning a higher HR is needed. On the other hand, when the stress ratio is high, adjustment factors as low as 0.9 would be more suitable to assess the cavability of the rock mass. If the joint sets are dipping away from the horizontal and vertical, there will be a need for a larger HR to initiate caving since the cave back is more stable for this structural arrangement. Consequently, adjustments to the above one would be suggested for these cases.

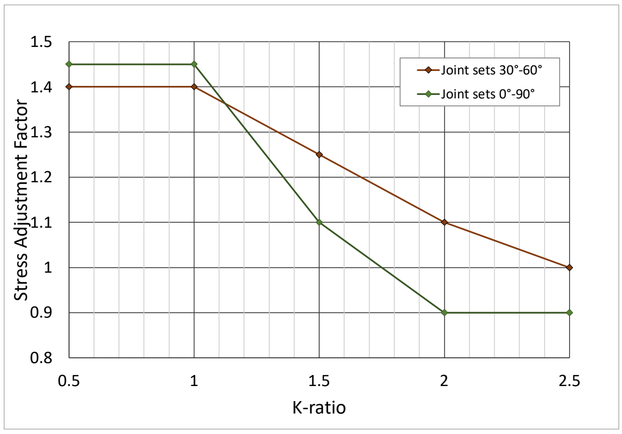

Figure 14 Adjustment factors by stresses for the MRMR calculation using Laubscher cavability chart.

Since all the models used for this study were set at the same depth, Figure 15 illustrates the importance of considering this parameter as an essential factor when evaluating cavability. It was found that lower-depth scenarios under a high K-ratio present a poorer match with Laubscher's curve, and a more detailed assessment should be incorporated into the analysis for these cases. This means that the adjustments presented in this section should be only considered for conditions similar to those modelled in this study.

5 CONCLUSIONS

The initial results of the 2D-FDEM models showed sensitivity to some of the input parameters used to define the rock masses. For example, unreliable crack initiation was observed using Mohr-Coulomb tensile strength without calibration. Similar case was observed when analyzing the Young's modulus for the poorest rock mass. This factor should be considered when modelling rock masses based on empirical correlations and calibrated with real data whenever possible.

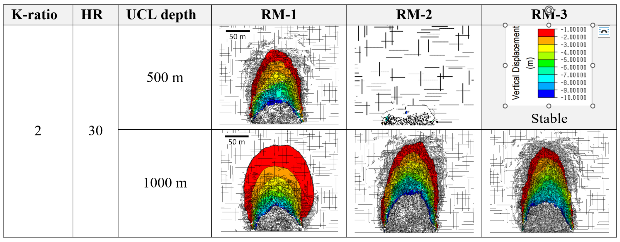

Figure 15 FDEM models comparing the effect of UCL depth for different rock masses under the same stress ratio and DFN1.

The different structural arrangements were incorporated into the FDEM coupling with a DFN model. This enabled the analysis of multiple structural settings in a sensitivity analysis combined with various stress regimes. The study showed that joints dipping with low angle (sub-horizontal) favour cavability, especially when combined with a sub-vertical joint set and high stresses, where crack initiation is more dominant in brittle rock masses.

The models using DFN1, showed vertical cave back propagation. Conversely, models using DFN2 exhibited a deviation of the cave back and deformation around it towards the direction of joint dipping. This cave back response could directly impact several aspects of a caving project, such as dilution and location of the subsidence crater when the cave breaks through the ground surface, among others.

When the results of the sensitivity analysis were compared with the empirical cavability chart, a poor correlation was found for the models under low-stress ratios, while a better match was observed for high stresses. Based on these results, two stress adjustment factor curves have been generated, which could be applied to conditions similar to those modelled in this work. This is based solely on conceptual models using the exact curves from Laubscher's chart; therefore, further validation with accurate data is required.

Empirical approaches, such as Laubscher's chart, were defined for conditions different from those that current projects are facing. This must be used cautiously, and the conditions must be evaluated case by case. As proved, its adjustment factors can change the results considerably depending on particular rock mass conditions. Therefore, as the stage of projects advances and a better understanding of the rock mass properties becomes available, a critical review of the initial predictions must be compared with detailed modelling. For this purpose, FDEM seems a good alternative.

ACKNOWLEDGEMENT

The authors acknowledge the Mitacs program and SRK Consulting for the support of this research and Rockfield (UK) for the ELFEN license.

REFERENCES

Bieniawski, Z. T. (1989). Engineering rock mass classifications: a complete manual for engineers and geologists in mining, civil, and petroleum engineering. New York, NY: Wiley.

Diering, J. A. C. & Laubscher, D. (1987). Practical approach to the mass mining numerical stress analysis. *Transactions of the Institution of Mining and Metallurgy*, Section A: Minerals Industry 96:A179–A188.

Elmo, D. (2006). Evaluation of a Hybrid FEM/DEM Approach for Determination of Rock Mass Strength Using a Combination of Discontinuity Mapping and Fracture Mechanics Modelling, with Particular Emphasis on Modelling of Jointed Pillars. PhD Thesis. Camborne School of Mines, University of Exeter.

Elmo, D., Farahmand, K., Rogers, S., Veltin, K. & Lett, J. (2022). An effective numerical method to understand different aspects of cave preconditioning. International Symposium on Block and Sublevel Caving (Caving 2022), 1337–1350.

Elmo, D., O'Connor, C., Vyazmensky, A., Stead, D., Dunbar, S., Eberhardt, E., Scoble, M. & Moss, A. (2007). Integrated modelling of subsidence mechanisms and impacts due to mine caving. 109th CIM Annual General Meeting Energy & Mines Conference, Montreal, Canada.

Elmo, D., Rogers, S., Beddoes, R. & Catalan, A. (2010). An integrated finite/discrete element method – discrete fracture network synthetic rock mass approach for modelling surface subsidence associated with panel cave mining at the Cadia East underground project. Proceedings of the 2nd International Symposium on Block and Sublevel Caving (Caving 2010), 167–179.

Elmo, D., Stead, D. & Rogers, S. (2008). Quantitative analysis of a fractured rock mass using a discrete fracture network approach: Characterization of natural fragmentation and implications for current rock mass classification systems. Proceedings of the 5th International Conference and Exhibition on Mass Mining (MassMin2008), Luleå University of Technology, Luleå, pp. 1023–1032.

Flores, G. & Karzulovic, A. (2003). Geotechnical guidelines for transitioning from open pit to underground mining: Caving propagation guidelines. Julius Kruttschnitt Mineral Research Centre, The University of Queensland, Brisbane, Australia.

Hoek, E. & Brown, E. T. (1997). Practical estimates of rock mass strength. *International Journal of Rock Mechanics and Mining Sciences*, 34(8), 1165–1186.

Hoek, E., Carranza-Torres, C. & Corkum, B. (2002). Hoek-Brown failure criterion-2002 edition. In Proceedings of the Fifth North American Rock Mechanics Symposium. Toronto, Canada. pp. 267-273.

Hoek, E., Carter, T. G. & Diederichs, M. S. (2013). Quantification of the geological strength index chart. In Proceeding of the 47th US Rock Mechanics/Geomechanics Symposium.

Hoek, E., & Diederichs, M. S. (2006). Empirical estimation of rock mass modulus. *International Journal of Rock Mechanics and Mining Sciences*, 43(2), 203–215.

Karzulovic, A. (2001). Altura de roca primaria en minería por panel caving. Estudio DT-CG-01-002. División El Teniente, Codelco. Santiago, Chile.

Kendorski, F. S. (1978). The cavability of ore deposits. *Mining Engineering*, 30(6): 628-631.

Klerck, P. A. (2000). The finite element modelling of discrete fracture in quasi-brittle materials. PhD Thesis. Swansea University.

Laubscher, D. (1975). Class distinction in rock masses. Coal, Gold Base Miner South Africa, 23(6):37–50.

Laubscher, D. (1990). A geomechanics classification system for the rating of rock mass in mine design. *Journal of the Southern African Institute of Mining and Metallurgy*, 90(10):257–273.

Laubscher, D. (1994). Cave mining-the state of the art. *Journal of the Southern African Institute of Mining and Metallurgy*, 94(10):279–293.

Laubscher, D. (2000). A Practical Manual on Block Caving: Julius Kruttschnitt Mineral Research Centre, The University of Queensland.

Laubscher, D. & Jakubec, J. (2001). The MRMR rock mass rating classification for jointed rock masses. In W. A. Hustrulid & R. L. Bullock (Eds.), Underground Mining Methods - Engineering Fundamentals and International Case Studies. Society for Mining, Metalurgy, and Exploration.

Lorig, L., Gibson, W., Alvial, J. & Cuevas, J. (1995). Gravity flow simulations with the particle flow code (PFC). *ISRM News Journal*, 3(1), 18-24.

Mawdesley, C. (2002). Predicting cave initiation and propagation in block caving mines. PhD Thesis. University of Queensland, Brisbane.

Pine, R. J., Owen, D. R. J., Coggan, J. S. & Rance, J. M. (2007). A new discrete modelling approach for rock masses. *Geotechnique*. 57(9): 757-766.

Rockfield. (2011). ELFEN 4.4 Explicit Manual (4.4.1). Rockfield Software Ltd. Retrieved from https://www.rockfieldglobal.com.

Shapka-Fels, T. (2022). Numerical analysis of the geomechanical interaction between open pit and cave mining using the hybrid finite-discrete element method. MASc. Thesis. University of British Columbia,Vancouver.

Suzuki, K. (2019). Development of a rock mass classification framework for caveability prediction. PhD Thesis. School of Mining Engineering, UNSW Sydney, Sydney.

Trueman, R. & Mawdesley, C. (2003). Predicting cave initiation and propagation. *CIM Bulletin* 96(1071):54–59.

Vyazmensky, A. (2008). Numerical Modelling of Surface Subsidence Associated with Block Cave Mining Using a Finite Element / Discrete Element Approach. PhD Thesis. Simon Fraser University.

WSP. (2023). FracMan Software v 8.0. FracMan Technology Group. Retrieved from http//:www.fracman.com/.